



1 **Do phenomenological dynamical paleoclimate models have physical similarity**  
2 **with Nature? Seemingly, not all of them do.**

3 Mikhail Y. Verbitsky<sup>1,2</sup> and Michel Crucifix<sup>2</sup>

4 <sup>1</sup>Gen5 Group, LLC, Newton, MA, USA

5 <sup>2</sup>UCLouvain, Earth and Life Institute, Louvain-la-Neuve, Belgium

6  
7 Correspondence: Mikhail Verbitsky (verbitskys@gmail.com)

8  
9 **Abstract.** Phenomenological models may be impressive in reproducing empirical time series but this is  
10 not sufficient to claim physical similarity with Nature until comparison of similarity parameters is  
11 performed. We illustrated such a process of diagnostics of physical similarity by comparing the  
12 phenomenological dynamical paleoclimate model of Ganopolski (2023), the van der Pol model (as used  
13 by Crucifix, 2013), and the model of Leloup and Paillard (2022) with the physically explicit Verbitsky *et*  
14 *al* (2018) model that played a role of a reference dynamical system. We concluded that phenomenological  
15 models of Ganopolski (2023) and of Leloup and Paillard (2022) may be considered to be physically  
16 similar with the proxy parent dynamical system in some range of parameters, or in other words they may  
17 be derived from basic laws of physics under some reasonable physical assumptions. We have not been  
18 able to arrive to the same conclusion regarding the van der Pol model. Though developments of better  
19 proxies of the parent dynamical system should be encouraged, we nevertheless believe that the  
20 diagnostics of physical similarity, as we describe it here, should become a standard procedure to delineate  
21 a model that is merely a statistical description of the data, from a model that can be claimed to have a link  
22 with known physical assumptions.

23  
24 **1. Introduction.**

25 A mathematical model that is constructed to understand a physical phenomenon must be simple  
26 enough, otherwise the interpretation of the modeling results may be as difficult as the interpretation of  
27 direct observations. In that regard, even most sophisticated space-resolving models of global climate  
28 provide, indeed, a simplified picture of the phenomenon, but a much more drastic degree of simplification  
29 is required when we study climate on timescales of tens of thousands of years. Faced with this challenge,  
30 Barry Saltzman used to be a proponent of the phenomenological approach “through the construction of  
31 low-order models in which the full behavior is projected onto the dynamics of a reduced number of  
32 ...highly aggregated variables...” (Saltzman, 2002). Phenomenological models of paleoclimate variability  
33 have routinely been used to explain certain characteristics of glacial-interglacial cycles (e.g., Saltzman  
34 and Maasch, 1991, Saltzman and Verbitsky, 1992, 1993, 1994, Paillard, 1998, Tziperman et al, 2006,  
35 Crucifix, 2013, Kaufmann and Pretis, 2021, Talento and Ganopolski, 2021, Leloup and Paillard, 2022,  
36 Ganopolski, 2023). The core principle of the phenomenological approach is to fit model-produced time  
37 series to the observational time series. When this goal is achieved, it is tacitly assumed that there must be  
38 some physical similarity between the phenomenological model and Nature. We believe though that the  
39 assumption of physical similarity with Nature can be more rigorously challenged before the implications  
40 of a phenomenological model are accepted.

41 In fluid dynamics, for example, the concept of physical similarity is the cornerstone of any judgement  
42 built on model experimentations. Classical similarity parameters, which emerge from the analysis of  
43 fundamental conservation laws, like the Reynolds number, the Peclet number, the Euler number, etc.,  
44 quantify the relative importance of different aspects of fluid flow. For an experimental or a numerical  
45 model to be relevant, it should have quantitatively the same similarity parameters as those of the natural  
46 phenomenon being considered. We will now apply this concept of physical similarity to dynamical  
47 paleoclimate systems.

48 As physicists, we might want to describe a phenomenon such as ice ages as “emerging from  
49 fundamental laws”. However, the fundamental laws that we know in physics dictate interactions between



50 particles. Perhaps one of the greatest challenges of the physical approach to complex systems is to explain  
51 how Nature organizes billions of billions of particles in interaction to generate some predictable behavior  
52 even on very long time scales such as, precisely, glacial-interglacial cycles. The methods of statistical  
53 physics tell us how to define macroscopic variables to describe the collective behavior of particles  
54 submitted to a conservation constraint, and how the phenomenon of dissipation emerges as a consequence  
55 of statistical mixing in a chaotic system. Dynamical system's theory tell us why we mainly see the most  
56 unstable modes of a system (Haken, 2006) and how time scale separation assumptions allows us to focus  
57 on a subset of the system's variables. In a nutshell, the theories of mathematical and statistical physics  
58 make it legitimate to assume that there is a natural parent dynamical system with much fewer degrees of  
59 freedom than Avogadro's number, and which has generated the phenomenon that we see.

60 What "much fewer" means is not a straightforward matter. It depends on what we describe as the  
61 phenomenon, and how fine-grained this description is. For example, the successions of glacial-interglacial  
62 cycles and the timing of deglaciations appear to follow fairly simple, predictable rules (Tzedakis et al.,  
63 2017). Hence, it is legitimate to assume that the physical parent dynamical system, which dictates the  
64 evolution of the macroscopic state of climate at the orbital time scale, can be reduced to a small number  
65 of degrees of freedom.

66 Specifically, we may suggest that this parent dynamical system is governed by  $n$  physical parameters  
67  $a_i$  such that a dependent variable of interest,  $x$ , can be expressed as function

68  
69 
$$x = \varphi(a_1, a_2, \dots, a_i, \dots, a_n) \quad (1)$$

70 If  $k$  parameters of  $a_1, a_2, \dots, a_i, \dots, a_n$  are parameters with independent dimensions, then, according to  $\pi$ -  
71 theorem (Buckingham, 1914), in the dimensionless form, the phenomenon (1) can be described by  
72  $m = n - k$  adimensional similarity parameters  $\Pi_1, \Pi_2, \dots, \Pi_i, \dots, \Pi_m$ :

73 
$$\Pi = \Phi(\Pi_1, \Pi_2, \dots, \Pi_i, \dots, \Pi_m) \quad (2)$$

74 Two physical phenomena have physical similarity if both of them are described in the adimensional  
75 form by the same function  $\Phi(\Pi_1, \Pi_2, \dots, \Pi_i, \dots, \Pi_m)$  and have identical numerical values of similarity  
76 parameters  $\Pi_1, \Pi_2, \dots, \Pi_i, \dots, \Pi_m$ , though numerical values of the governing parameters  
77  $a_1, a_2, \dots, a_i, \dots, a_n$  may be different (e.g., Barenblatt, 2003).

78 As we have already mentioned, our knowledge about a parent dynamical system is suggested to us by  
79 the presence of empirical time series. It means that one of the similarity parameters, let say  $\Pi_1$ , is  
80 adimensional time  $\frac{t}{\tau}$  ( $t$  and  $\tau$  are dimensional time and a timescale, correspondingly), and all other  
81 parameters  $\Pi_2, \dots, \Pi_i, \dots, \Pi_m$  are fixed to specific values. Hence, an experimental time series (neglecting  
82 measure errors) can be described as

83  
84 
$$\Pi = \Phi\left(\frac{t}{\tau}, \Pi_2, \dots, \Pi_i, \dots, \Pi_m\right) \quad (3)$$

85 If we created a model dynamical system such that it is governed by  $p$  governing parameters  $b_i$

86 
$$x = \psi(b_1, b_2, \dots, b_i, \dots, b_p) \quad (4)$$

87 and  $r$  parameters of  $b_1, b_2, \dots, b_i, \dots, b_p$  are parameters with independent dimensions, then, again,  
88 according to  $\pi$ -theorem, in the dimensionless form, the model can be described by  $q = p - r$   
89 adimensional similarity parameters  $\pi_1, \pi_2, \dots, \pi_i, \dots, \pi_q$ :

90 
$$\pi = \Psi(\pi_1, \pi_2, \dots, \pi_i, \dots, \pi_q) \quad (5)$$

91 For a specific time series, and for a fixed set of parameters  $\pi_2, \dots, \pi_i, \dots, \pi_q$ , the model (5) can be  
92 presented as



93 
$$\pi = \Psi \left( \frac{t}{\tau}, \pi_2, \dots, \pi_i, \dots, \pi_q \right) \quad (6)$$

94 The essence of the phenomenological approach is to fit the function  $\Psi \left( \frac{t}{\tau}, \pi_2, \dots, \pi_i, \dots, \pi_q \right)$  to the  
95 function  $\Phi \left( \frac{t}{\tau}, \Pi_2, \dots, \Pi_i, \dots, \Pi_m \right)$  under the “best” set of parameters  $\pi_2, \dots, \pi_i, \dots, \pi_q$ , i.e. to equate the  
96 model time series  $\Psi \left( \frac{t}{\tau}, \pi_2, \dots, \pi_i, \dots, \pi_q \right)$  and the natural, empirical, time series  $\Phi \left( \frac{t}{\tau}, \Pi_2, \dots, \Pi_i, \dots, \Pi_m \right)$ :

97 
$$\Psi \left( \frac{t}{\tau}, \pi_2, \dots, \pi_i, \dots, \pi_q \right) = \Phi \left( \frac{t}{\tau}, \Pi_2, \dots, \Pi_i, \dots, \Pi_m \right) \quad (7)$$

98 It is obvious that even if the goal (7) is achieved at every  $\frac{t}{\tau}$ -point, we still cannot claim the model (6)  
99 to be physically similar to “Nature” (3) until we prove that  $\pi_i = \Pi_i$ , i.e.,  $\pi_i$ -physics in the model is as  
100 significant as the  $\Pi_i$ -physics of Nature. Simply speaking, merely *matching a proposed phenomenological*  
101 *model with empirical data does not make a case for physical similarity* because it does not provide an  
102 evidence that it happens for the right reason, the reason being the similarity parameters of the right value,  
103 i.e.,  $\pi_i = \Pi_i$ .

104 But how can we compare  $\pi_i$ -physics of the phenomenological model and  $\Pi_i$ -physics of Nature if the  
105 phenomenological models are not derived from the laws of physics? Though, indeed, phenomenological  
106 models have not been derived from the laws of physics, they are not completely ignorant of the physical  
107 content: they still have a physical, measurable variable, time; they also have orbital and terrestrial  
108 forcings as well as positive and negative feedbacks. If the parent dynamical system was formulated in  
109 terms of similarity parameters formed by the ratios of timescales and by the ratios of the forcings’ and  
110 feedbacks’ amplitudes, then the comparison with phenomenological models that also use time scales and  
111 forcing and feedback ratios would be possible. The VCV18 model (Verbitsky et al, 2018), is one such  
112 candidate (a proxy) for a parent dynamical system. VCV18 was *derived* from the scaled mass- and heat-  
113 balance equations of the non-Newtonian ice flow. Next, we will derive scaling laws and similarity  
114 parameters for three phenomenological models: (a) the model of Ganopolski (2023); (b) van der Pol  
115 model as it has been described by Crucifix (2013); and (c) the model of Leloup and Paillard (2022);  
116 G23, VDP and LP22, thereafter, respectively. Each of these models produces a specific function  
117  $\Psi(\pi_1, \pi_2, \dots, \pi_i, \dots, \pi_q)$ . We then compare functions  $\Psi(\pi_1, \pi_2, \dots, \pi_i, \dots, \pi_q)$  of these models with the  
118 corresponding function  $\Phi(\Pi_1, \Pi_2, \dots, \Pi_i, \dots, \Pi_m)$  provided by VCV18 to recognize or reject the hypothesis  
119 of physical similarity with a proxy for the parent dynamical system.

120 Certainly, we cannot expect that the time series produced by G23, VDP, and LP22 models and by the  
121 VCV18 model are identical, and therefore these models will not be physically similar in the most rigorous  
122 sense of the equation (7). We will demonstrate though that the answer to the physical-similarity question  
123 is insightful if our dependent variable of interest  $x$  is not necessarily a time series but a time-independent  
124 attribute such as the period of glacial rhythmicity. All models of this study reproduce equally well ~100-  
125 kyr period of the late Pleistocene glaciations. We will now evaluate if the similarity parameters involved  
126 in the corresponding equations (7) are quantitatively the same.

127

## 128 2. Method

129

### 130 2.1 VCV18 model as a proxy for a parent dynamical system.

131

132 Deriving a low-order dynamical paleoclimate model that may be considered as a candidate (a proxy)  
133 parent dynamical system is not a trivial exercise. The “low-order” challenge means that out of the  
134 multitude of physical phenomena involved only few should be recognized as dominant ones, and the  
135 “dynamical” challenge means that the space-resolving properties should be sensibly reduced to some  
136 integrated variables. Accordingly, in developing VCV18 proxy parent dynamical system, we first



137 assumed that ice ages can be explained by only two components of the global climate system, continental  
 138 ice sheets and the ocean representing the rest of the climate. For an ice sheet we adopted mass,  
 139 momentum, and heat conservation equations of a “thin” layer of homogeneous non-Newtonian ice, and  
 140 the rest of the climate was represented by the energy-balance equation. To migrate from the three-  
 141 dimensional to dynamical equations we used scaling analysis that provides simple mathematical  
 142 statements that are consistent with the original physics. Accordingly, the VCV18 dynamical model of the  
 143 ice-climate system is defined by the following set of equations:

$$144 \quad \frac{dS}{dt} = \frac{4}{5} \zeta^{-1} S^{3/4} (\hat{a} - \varepsilon F - \kappa \omega - c\theta) \quad (8)$$

$$145 \quad \frac{d\theta}{dt} = \zeta^{-1} S^{-1/4} (\hat{a} - \varepsilon F - \kappa \omega) \{ \alpha \omega + \beta [S - S_0] - \theta \} \quad (9)$$

$$146 \quad \frac{d\omega}{dt} = -\gamma [S - S_0] - \frac{\omega}{\tau} \quad (10)$$

147

148 Here,  $S$  ( $\text{m}^2$ ) is the area of glaciation,  $\theta$  ( $^{\circ}\text{C}$ ) is the basal ice-sheet temperature, and  $\omega$  ( $^{\circ}\text{C}$ ) is the global  
 149 temperature of the rest of the climate. Equation (8) represents global ice balance  $\frac{d(HS)}{dt} = AS$ , where the  
 150 ice thickness  $H$  is determined from the thin-layer approximation of ice flow,  $H = \zeta S^{1/4}$ ,  $\zeta$  is dimensional  
 151 profile factor (Verbitsky and Chalikov, 1986) and  $A = \hat{a} - \varepsilon F - \kappa \omega - c\theta$  is the surface mass influx.  
 152 Equation (9) describes vertical ice temperature advection with a time scale  $H/(\hat{a} - \varepsilon F - \kappa \omega)$ , and  
 153 equation (10) is the global energy-balance equation. The parameter  $\hat{a}$  ( $\text{m s}^{-1}$ ) is the snow precipitation  
 154 rate;  $F$  is normalized external forcing, i.e., mid-July insolation at  $65^{\circ}\text{N}$  (Berger and Loutre, 1991) of the  
 155 amplitude  $\varepsilon$  ( $\text{m s}^{-1}$ );  $\kappa \omega$  represents fast positive feedback from the global climate on ice-sheet mass  
 156 balance;  $c\theta$  is the ice discharge due to ice-sheet basal sliding incorporating (both delayed due to the  
 157 vertical temperature advection) positive feedback from the global temperature,  $\alpha \omega$ , and a negative  
 158 feedback of basal temperature reaction to the changes of ice geometry  $\beta [S - S_0]$ . Further,  $-\gamma [S - S_0]$  is  
 159 external forcing for global temperature (e.g., albedo);  $\kappa$  ( $\text{m s}^{-1} \text{ } ^{\circ}\text{C}^{-1}$ ),  $c$  ( $\text{m s}^{-1} \text{ } ^{\circ}\text{C}^{-1}$ ),  $\alpha$  (adimensional),  $\beta$   
 160 ( $^{\circ}\text{C m}^{-2}$ ) and  $\gamma$  ( $^{\circ}\text{C m}^{-2} \text{ s}^{-1}$ ) are sensitivity coefficients;  $S_0$  ( $\text{m}^2$ ) is a reference glaciation area; and  $\tau$  (s) is the  
 161 global-temperature timescale.

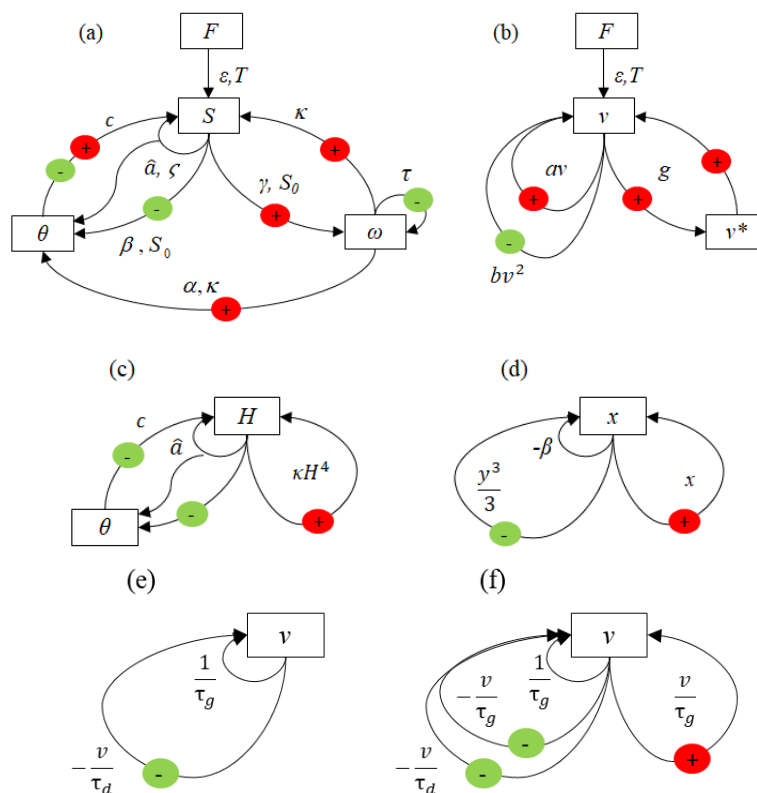
162 Schematically, the dynamical system (8) – (9) is shown in Fig. 1(a). It can be seen that the dynamics  
 163 of the VCV18 system is defined by the amplitude and periodicity of the orbital forcing,  $\varepsilon$ ,  $T$ , by the  
 164 terrestrial forcing  $\hat{a}$ , and by three feedback loops: the fast positive feedback,  $-\kappa \omega$ , and by two delayed,  
 165 positive and negative feedbacks, combined in the term  $-c\theta$ . The dimensional analysis of the VCV18  
 166 model has been performed previously (Verbitsky and Crucifix, 2020, 2021, Verbitsky, 2022a). It was  
 167 revealed that its large-scale periodicity is generally governed by two dimensionless parameters: the ratio  
 168 of the astronomical forcing amplitude  $\varepsilon$  to the terrestrial ice-sheet mass influx,  $\Pi_2 = \varepsilon/\hat{a}$  and the so-called  
 169  $V$ -number,  $\Pi_3 = V$  that is the ratio of amplitudes of time-dependent positive and negative feedbacks.  
 170 Specifically, the period  $P$  of the VCV18 system response to the astronomical forcing of period  $T$  is of the  
 171 form (hereafter called the “ $P$ -scaling law”):

$$172 \quad \frac{P}{T} = \Phi \left( \frac{\varepsilon}{\hat{a}}, V \right) \quad (11)$$

173 For  $T = 40$  kyr,  $\frac{\varepsilon}{\hat{a}} = 1.4$ ,  $V = 0.7$ ,  $\Phi = 2$  (obliquity-period doubling). The corresponding time series and  
 174 positive-versus-negative feedback evolution are shown in Fig. 2(a, b).



175

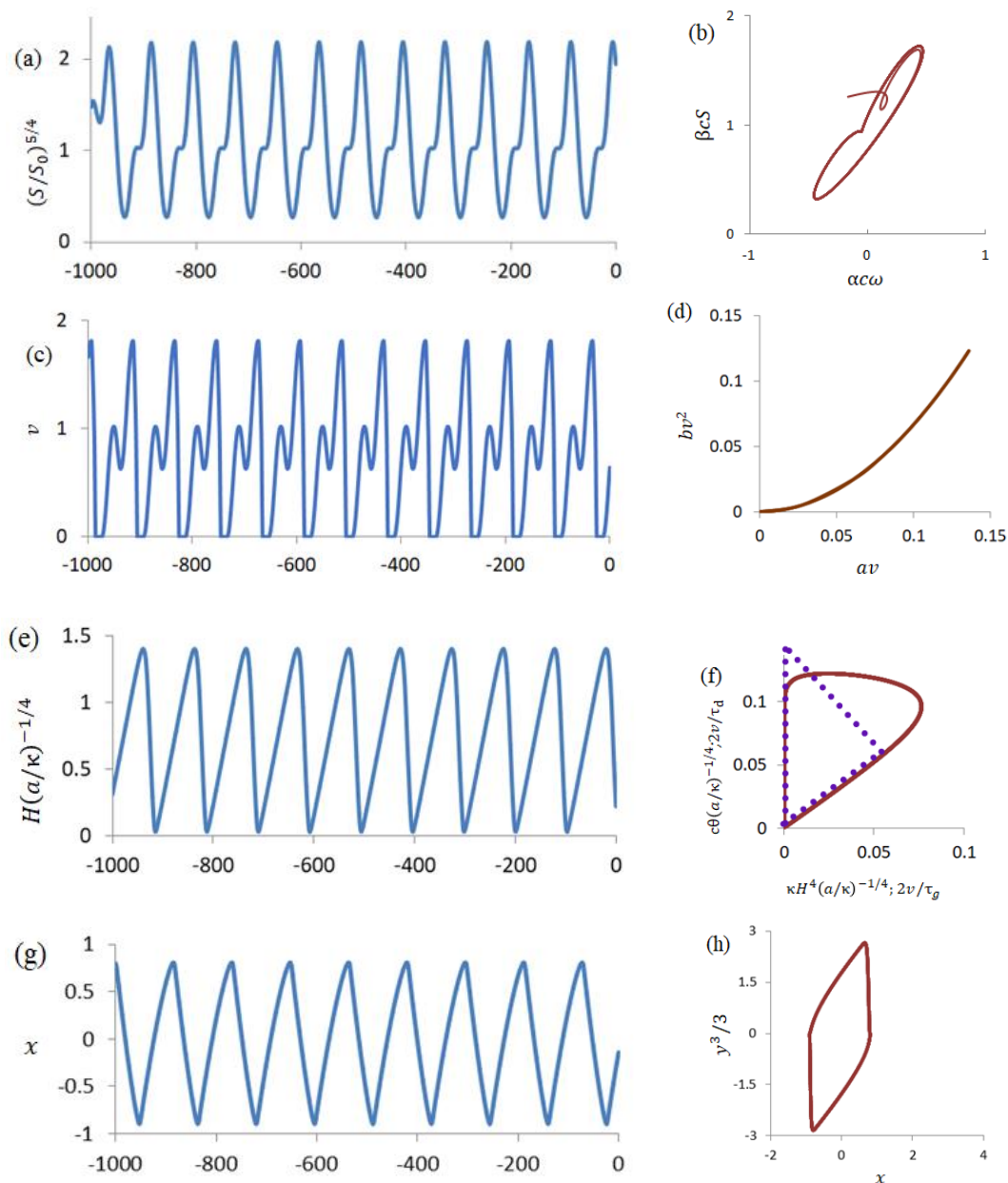


176

177 **Figure 1.** (a) The parent dynamical system VCV18 (Eqs. 8–10). Red circles mark positive feedback loops  
 178 and green circles mark negative feedback loops; (b) The same for the G23 phenomenological model (Eqs.  
 179 12-13); (c) The same for simplified system VCV18-1 (Eqs. 22–23); (d) The same for VDP model (Eqs.  
 180 30-31); (e) The same for LP22 model (Eqs. 37-38),  $I = 0$ ; (f) The same for LP22 model (Eqs. 44-45);



181



182

183

184

185

186

187

**Figure 2.** Time series (kyr BP) and corresponding positive-*vs*-negative feedback loops: (a, b) VCV18 (Eqs. 8–10),  $\left(\frac{S}{S_0}\right)^{5/4}$  is normalized ice volume; (c, d) G23 (Eqs. 12–13); (e, f) VCV18-1 (Eqs. 22–23); all variables are normalized by characteristic ice thickness,  $H' = (\hat{a}/\kappa)^{1/4}$ , the dotted triangle corresponds to LP22 (Eqs. 37–38) without astronomical forcing; (g, h) VDP (Eqs. 30–31).



188 **2.2 G23 model.**

189 The G23 model describes evolution of global ice volume  $v$  (adimensional) as a response to orbital forcing  
 190  $\varepsilon F$  ( $F$  is normalized external forcing of the amplitude  $\varepsilon$ ):

191 
$$\frac{dv}{dt} = \frac{av - bv^2 - \varepsilon F + d}{1 - \delta g v^*}$$
 (12)

192  
 193 
$$v^* = \frac{1}{T^*} \int_{t-T^*}^t v(t') dt'$$
 (13)

194  
 195 The term  $\delta g v^*$  represents an additional positive feedback activated ( $\delta = \delta_1 = 1$ ) when  $\frac{dv}{dt} < 0$ .  
 196 When  $\frac{dv}{dt} \geq 0$ ,  $\delta = \delta_2 = 0$ . Graphically, the dynamical system (12) – (13) is shown in Fig. 1(b). We  
 197 observe that the dynamics of the G23 system is, like VCV18, defined by the amplitude and periodicity of  
 198 the orbital forcing,  $\varepsilon, T$  and by three feedback loops: two positive feedbacks,  $av, g v^*$  and by one negative  
 199 feedback,  $-bv^2$ . Unlike VCV18, though, all feedbacks are instantaneous. We now review how these  
 200 differences may be reflected in the corresponding  $P$ -scaling law.

201 For the purpose of dimensional analysis, we consider Eqs. (12) – (13) in dimensional form assuming  
 202 the following dimensions for variables and parameters involved:  $t$  (s),  $v$  ( $\text{m}^3$ ),  $a$  ( $\text{s}^{-1}$ ),  $b$  ( $\text{m}^{-3}\text{s}^{-1}$ ),  $\varepsilon$  ( $\text{m}^3\text{s}^{-1}$ ),  $F$   
 203 is an adimensional function of the period  $T$  (s),  $d$  ( $\text{m}^3\text{s}^{-1}$ ),  $\delta_1, \delta_2$  (adimensional),  $g$  ( $\text{m}^{-3}$ ),  $v^*$  ( $\text{m}^3$ ). The  
 204 period of the system response to the astronomical forcing is then a function of the following governing  
 205 parameters:

206  
 207 
$$P = \psi(a, b, \varepsilon, T, d, \delta_1, \delta_2, g)$$
 (14)

208  
 209 For more explicit physical interpretation, instead of the parameter  $b$ , we will use parameter  $\hat{a} = \frac{a^2}{b}$ ,  
 210 ( $\text{m}^3\text{s}^{-1}$ ), which is the mean growth rate. Also, for the reference values of parameters, provided by  
 211 G23,  $d \ll \varepsilon$ , and, lastly,  $\delta_1, \delta_2$  are constant. Therefore we can re-write (14) as:

212  
 213 
$$P = \psi(a, \hat{a}, \varepsilon, T, g)$$
 (15)

214  
 215 If we choose  $\hat{a}, T$  as parameters with independent dimensions, then according to  $\pi$ -theorem:

216  
 217 
$$\frac{P}{T} = \Psi\left(\frac{\varepsilon}{\hat{a}}, T a, T g \hat{a}\right)$$
 (16)

218  
 219 Let us now determine the  $V$ -number for G23 as the ratio of amplitudes of time-dependent positive and  
 220 negative feedbacks. Obviously, such ratio should be completely defined by the internal (terrestrial) G23  
 221 properties and therefore:

222  
 223 
$$V = \lambda(a, b, g)$$
 (17)

224  
 225 If we choose  $a$  and  $b$  as parameters with independent dimensions, then according to  $\pi$ -theorem:

226  
 227 
$$V = \Lambda\left(\frac{ga}{b}\right)$$
 (18)

228  
 229 We can also express  $g$  as a function of  $V$ :

230  
 231 
$$\frac{ga}{b} = \Lambda^{-1}(V)$$
 (19)

232



233 Accordingly, the  $P$ -scaling law of G23 can be written as:

234

$$235 \frac{P}{T} = \Psi \left[ \frac{\varepsilon}{\hat{a}}, Ta, Ta\Lambda^{-1}(V) \right] \quad (20)$$

236

237 or

238

$$239 \frac{P}{T} = \Psi \left( \frac{\varepsilon}{\hat{a}}, \frac{T}{\tau}, V \right); \tau = 1/a \quad (21)$$

240 We see that the scaling law (21) is different from the scaling law (11) because the  $\Psi$  – function of (21)  
 241 depends on  $T$  unlike the  $\Phi$  – function of (11). There are only two scenarios for orbital periods to escape  
 242 the  $\Psi$  – function (or the  $\Phi$  – function) in a scaling law. First, they may be excluded from the governing  
 243 equations when the main period of system’s variability is attributed to the internal, terrestrial, physics.  
 244 This is the case for VDP and LP22 models that will be considered later, but, definitely, it is not applicable  
 245 neither to G23 nor VCV18. The second scenario occurs when a system incorporates multiple parameters  
 246 encoding different time scales. The interplay of these parameters may create a situation when  $T$ -  
 247 dependent similarity parameters form jointly a  $T$ -independent conglomerate similarity parameter, giving a  
 248 system the so-called property of incomplete similarity (Barenblatt, 2003). This property has been  
 249 discovered for VCV18 (Verbitsky, 2022a). Indeed, it has two major timescales of the same order of  
 250 magnitude, the timescale of ice growth and the timescale of the vertical temperature advection in the ice  
 251 sheet. As the result, the  $\Phi$  – function of the scaling law (11) does not depend on orbital period ( $\Phi = 2$   
 252 in the range of  $T = 35 - 60$  kyr). Contrarily, as we have already noted, G23 positive and negative feedbacks  
 253 are instantaneous, G23 single ice-growth timescale  $\tau \sim 1/a$  does not have a “counterpart” for an interplay,  
 254 and therefore the  $\Psi$  – function of (21) is period- $T$  dependent.

255 Specifically, for  $T = 40$  kyr,  $\frac{\varepsilon}{\hat{a}} = 1.6$ ,  $V = 1.1$ ,  $\Psi = 2$  (obliquity-period doubling). Hence, only for a  
 256 given quasi-periodic forcing, e.g., obliquity, VCV18 and G23 models appear physically similar in regards  
 257 of two similarity parameters,  $\frac{\varepsilon}{\hat{a}}$ , the ratio of the astronomical forcing amplitude  $\varepsilon$  to the growth rate  $\hat{a}$ ,  
 258 and in terms of the  $V$ -number. The corresponding time series and positive-versus-negative feedback  
 259 evolution are shown in Fig. 2 (c, d).

260

### 261 2.3 Simplified VCV18 model (VCV18-1) as a proxy for a parent dynamical system

262

263 The next phase of our study is devoted to two phenomenological models, VDP and LP22 that have  
 264 100-kyr auto-oscillations independently of orbital forcing. To make the diagnostics of physical similarity  
 265 possible, we have to further simplify VCV18 system with several, physically reasonable, assumptions:

- 266 (a) Since the global-temperature timescale in equation (10) is much faster than other timescales  
 267 (orbital, ice accumulation, and ice-temperature advection), we assume that global temperature is  
 268 an instantaneous function of the glaciation forcing,  
 269 (b) In equation (9), we assume  $\alpha = 0$  (for example, effect of increased global temperature is offset  
 270 by increased snow precipitation rate, see experiment D in the Appendix of VCV18), which  
 271 cancels the direct effect of climate on basal temperature,  
 272 (c) We rewrite equations (8) and (9) in terms of ice thickness  $H = \zeta S^{1/4}$ , and finally  
 273 (d) We attribute all system variability to terrestrial causes ( $\varepsilon = 0$ ).

274 The simplified dynamical system then takes the following form:

$$275 \frac{dH}{dt} = \hat{a} + \kappa H^4 - c\theta \quad (22)$$

276





$$277 \quad \frac{d\theta}{dt} = \frac{H^4 - \theta}{H/\hat{a}} \quad (23)$$

278

279 The physical meaning of all variables and governing parameters are the same as in equations (8) – (9), but  
 280 the numerical values and dimensions of some parameters and variables are, indeed, different. Specifically,  
 281  $t(s)$ ,  $H$  (m),  $\theta$  ( $m^4$ ),  $\hat{a}$  ( $m s^{-1}$ ),  $\kappa$  ( $m^{-3} s^{-1}$ ),  $c$  ( $m^{-3} s^{-1}$ ). The casual graph of the dynamical system (22) – (23) is  
 282 shown in Fig. 1 (c).

283 The period of system variability is a function of three governing parameters:

284

$$285 \quad P = \varphi(\hat{a}, \kappa, c) \quad (24)$$

286

287 If we choose  $\hat{a}, \kappa$  as parameters with independent dimensions, then according to  $\pi$ -theorem:

288

$$289 \quad \frac{P}{\tau} = \Phi\left(\frac{\kappa}{c}\right) \quad (25)$$

290

$$291 \quad \tau = (\hat{a}^3 \kappa)^{-1/4}$$

292

293 Parameters  $\hat{a}, \kappa, c$  lack in VDP and LP22 models, and therefore we transition to the  $V$ -number that must  
 294 be a function of the same  $\hat{a}, \kappa, c$  parameters:

295

$$296 \quad V = \lambda(\hat{a}, \kappa, c) \quad (26)$$

297

298 Since the  $V$ -number is adimensional, and  $\hat{a}, \kappa$  are parameters with independent dimensions, then  
 299 according to  $\pi$ -theorem:

300

$$301 \quad V = \Lambda(\kappa/c) \quad (27)$$

302

303 It also means that

304

$$305 \quad \frac{\kappa}{c} = \Lambda^{-1}(V) \quad (28)$$

306

307 and we can finally present the VCV18-1  $P$ -scaling law as:

308

$$309 \quad \frac{P}{\tau} = \Phi(V) \quad (29)$$

310

311 In other words, the  $P$ -scaling law of the VCV18-1 system is fully defined by the balance between positive  
 312 and negative feedbacks. For  $\tau = 50$  kyr,  $V = 0.63$ ,  $\Phi = 2$ . The corresponding 100-kyr-period auto-  
 313 oscillations of the system (22) – (23) and its positive-versus-negative feedback loop are shown in Fig. 2  
 314 (e, f).

## 315 2.4 VDP model

316 We now consider the VDP model, which is a variant of the historical van der Pol model (1922) used  
 317 by De Saedeleer et al. (2013) and Crucifix (2013) to study synchronization properties of ice ages.

$$318 \quad \frac{dx}{dt} = \frac{-\beta - y}{\tau} \quad (30)$$

$$319 \quad \frac{dy}{dt} = \frac{\alpha}{\tau} \left( y - \frac{y^3}{3} + x \right) \quad (31)$$



320 Here all variables and parameters, except time and timescale  $\tau$ , are adimensional. Variable  $x$  is a proxy for  
321 the glaciation, and variable  $y$  represents the rest of the climate. Since  $\frac{\tau}{\alpha} \ll \tau$ , for longer, glaciation-like  
322 processes, we can re-write equations (30) – (31) as:

$$323 \quad \frac{dx}{dt} = \frac{1}{\tau} \left( -\beta + x - \frac{y^3}{3} \right) \quad (32)$$

$$324 \quad y - \frac{y^3}{3} + x = 0 \quad (33)$$

325 The equation (33) defines the “critical manifold” (Guckenheimer et al, 2003). The system (32) – (33)  
326 describes VDP “slow” dynamics between two glacial-interglacial bifurcation points. To get VDP time  
327 series, we solve the non-idealized system (30) – (31), and we use the system (32) – (33) to visualize  
328 system’s positive,  $x$ , and negative,  $\frac{y^3}{3}$  feedbacks. Schematically, the dynamical system (30) – (31) is  
329 shown in Fig. 1 (d). The period of system (30) – (31) variability is the function of two governing  
330 parameters:

$$332 \quad P = \psi(\tau, \beta) \quad (34)$$

333 Only parameter  $\tau$  is dimensional, and therefore according to  $\pi$ -theorem:

$$334 \quad \frac{P}{\tau} = \Psi(\beta) \quad (35)$$

335 The amplitudes of VDP variables are defined by the critical manifold (33) that does not contain  
336 parameters  $\tau, \beta$  and therefore both  $x$ - and  $y$ -amplitudes do not depend on model parameters. Consequently  
337 the amplitudes of positive and negative feedbacks do not depend on them either. In fact, the  $x$ -amplitude  
338 in VDP model is always  $\sim 0.8$  and  $y$ -amplitude is always 2. Therefore the ratio of the amplitude of the  
339 positive feedback,  $x$ , to the amplitude of the negative feedback,  $\frac{y^3}{3}$ , is always  $V = 0.3$ . In summary:

$$341 \quad V = \text{const} \quad (36)$$

342

343 The property (36) makes VDP model to be fundamentally different from all other models in this  
344 study. In all other models, the  $V$ -number is the function of model’s governing parameters and, under  
345 different scenarios, it changes when parameters change. In the VDP model, the  $V$ -number is pre-defined  
346 by the model’s structure. Consequently, the scaling law (35) does not contain any  $V$ -number and thus it  
347 cannot match the scaling law (29). Therefore, *there is no physical similarity* between the VCV18-1 and  
348 the VDP models.

349 The auto-oscillations of the system (30) – (31) and positive-versus-negative feedback evolution are  
350 shown in Fig. 2 (g, h). For  $\tau = 50$  kyr and  $\beta = 0.3$ ,  $\Psi = 2.2$ . Fig. 2 (e) and Fig. 2 (g) show well why the  
351 phenomenological approach may be misleading. For the same internal timescale of 50 kyr, VCV18-1 and  
352 VDP models both produce asymmetrical (slow growth and fast retreat) glaciation time series with the  
353 respective periods  $P$  close to 100 kyr, but this occurs because of very different physics: in the VDP model  
354 the positive feedbacks are much weaker (as we already know,  $V = 0.3$ , always) than in the VCV18-1  
355 model ( $V = 0.63$ ). Most importantly, this discrepancy cannot be changed, because the VDP model is  
356 rigid in this regard.

357

## 358 2.5 LP22 model

359

360 The LP22 model is described by two differential equations, first, for the growing ice volume,



361 
$$\frac{dv}{dt} = -\frac{I}{\tau_i} + \frac{1}{\tau_g} \quad (37)$$

362 and another one for the diminishing ice volume

363 
$$\frac{dv}{dt} = -\frac{I}{\tau_i} - \frac{v}{\tau_d} \quad (38)$$

364 Here,  $v$  and  $I$  are normalized ice volume and astronomical forcing, correspondingly;  $\tau_i$ ,  $\tau_g$ , and  $\tau_d$  are  
 365 dimensional timescales. Additionally, if  $I < I_0$  the system switches from equation (38) to equation (37),  
 366 and if  $I + v > V_0$ , the system switches from equation (37) to equation (38). Though the original LP22  
 367 model does not consider its evolution without astronomical forcing, oscillations still occur when  $I = 0$  and  
 368 the equation-switching conditions are, correspondingly,  $v \leq V_1$  ( $V_1$  is the minimal, interglacial, volume)  
 369 and  $v \geq V_0$ . Schematically, the dynamical system (37) – (38) with  $I = 0$  is shown in Fig. 1 (e). The period  
 370 of auto-oscillations is a function of four parameters:

371  
 372 
$$P = \psi(V_0, \tau_g, V_1, \tau_d) \quad (39)$$

373 The parameter  $V_1 \ll V_0$  can be settled as a constant, therefore:

374 
$$P = \psi(V_0, \tau_g, \tau_d) \quad (40)$$

375 If we select  $\tau_g$  as an independent-dimension parameter, then according to  $\pi$ -theorem:

376 
$$\frac{P}{\tau_g} = \Psi(V_0, \tau_d/\tau_g) \quad (41)$$

377 The equation (37) describes a linear ice volume growth implying zero net feedback. This doesn't indicate  
 378 the absence of feedbacks. Indeed, if we are ready to accept that LP22 model is more than just a successful  
 379 fit to empirical data, then for the growing ice sheet, the equation (37) should be consistent with the  
 380 dimensional total mass balance

381  
 382 
$$\frac{dv}{dt} = \hat{a}S \quad (42)$$

383  
 384 i.e., changes of ice volume are equal to mass influx  $\hat{a}$  accumulated over its area  $S$ . If we multiply and  
 385 divide  $\hat{a}S$  by ice thickness  $H$ , the total mass balance (42) becomes

386  
 387 
$$\frac{dv}{dt} = \frac{v}{\tau_g} \quad (43)$$

388  
 389 where  $\tau_g = H/\hat{a}$ . The equation (43) tells us that the positive feedback  $\frac{v}{\tau_g}$  must be present in the growing  
 390 ice sheet: it relates to the area growth with thickness. Its absence in equation (37), therefore suggests that  
 391  $\hat{a}$  has another component that completely compensates for  $\frac{v}{\tau_g}$ , and yet another component that is inversely  
 392 proportional to  $S$  (e.g., continentality effect). Hence, the system (37) – (38) must be written as follows to  
 393 have physical meaning:

394  
 395 
$$\frac{dv}{dt} = \frac{1}{\tau_g} + \frac{v}{\tau_g} - \frac{v}{\tau_d} \quad (44)$$

396 
$$\frac{dv}{dt} = -\frac{v}{\tau_d} \quad (45)$$



397 Schematically, the dynamical system (44) – (45) is shown in Fig. 1 (f). The amplitude of the positive  
398 feedback is  $\frac{V_0}{\tau_g}$  and the amplitude of the negative feedback is  $\max\left\{\frac{V_0}{\tau_g}; \frac{V_0}{\tau_d}\right\}$ . Since  $\tau_g > \tau_d$ , the  $V$ -number  
399 therefore is equal to:  
400

$$401 \quad V = \frac{\tau_d}{\tau_g} \quad (46)$$

402 Accordingly, the  $P$ -scaling law (41) for LP22 model can be written as

$$403 \quad \frac{P}{\tau_g} = \Psi(V_0, V) \quad (47)$$

404 For example, for  $\tau_g = 50$  kyr,  $V_0 = 1.5$ ,  $V_1 = 0.2$ ,  $\tau_d = 20$  kyr, we get  $V = 0.4$  and  $\Psi = 2$ . As we  
405 have established before, for VCV18-1 model, for  $\tau = 50$  kyr,  $V = 0.63$ ,  $\Phi = 2$ . Therefore, we can talk  
406 about *physical similarity* between VCV18-1 and LP22 models in terms of the  $V$ -number.

407 The similarity between VCV18-1 and LP22 models becomes very visual in Fig. 2(f) describing the  
408 positive-versus-negative feedback loops. It can be observed that in VCV18-1 model, during much of ice  
409 growth, positive and negative feedbacks also completely compensate each other. In fact, we can consider  
410 LP22 model as being an approximation of the VCV18-1 feedback loop by a triangle. Indeed, the LP22  
411 positive and negative feedbacks compensate each other during ice advance and when the critical value of  
412  $v$  (i.e.,  $V_0$ ) is achieved, the system instantly migrates to the single dominant negative feedback. Simply  
413 speaking, these two models are as similar as the shape of the LP22 feedback-loop triangle in Fig. 2(f) is  
414 similar to the shape of the VCV18-1 feedback loop, since the  $V$ -number is the ratio of its horizontal  
415 dimension to its vertical dimension.

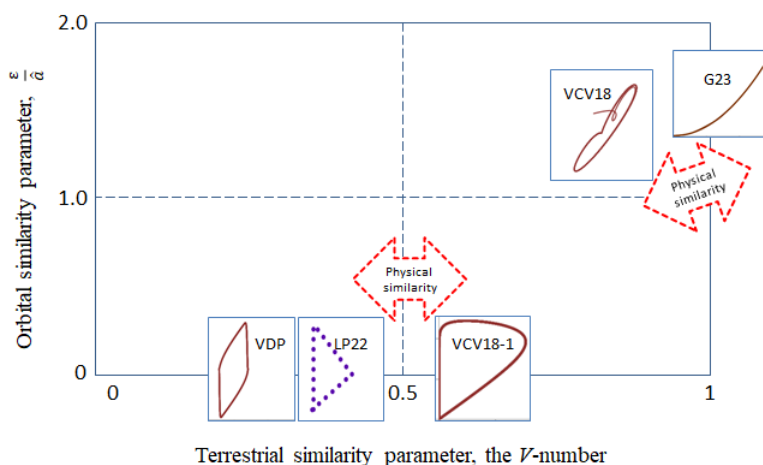
### 416 3. Conclusions

417 Nikolai Gogol would have said: “A magic apple tree may grow golden apples...but not pears”.  
418 Phenomenological models may not be bounded by a specific physics but they have to be consistent with  
419 the laws of physics. The concept of physical similarity is what allows us to be vigilant about such  
420 consistency. Accordingly, we started our presentation with the question: Are phenomenological  
421 dynamical paleoclimate models physically similar to Nature? We demonstrated that, though they may be  
422 remarkably accurate in reproducing empirical time series, this is not sufficient to claim physical similarity  
423 with Nature until similarity parameters are considered. We illustrated such a process of diagnostics of  
424 physical similarity by comparing three phenomenological dynamical paleoclimate models with the more  
425 explicit model that played the role of parent dynamical system. Though the nomination of the VCV18  
426 model to serve as a proxy of the parent dynamical system can, indeed, be questioned, and the  
427 developments of better proxies should be encouraged, we nevertheless believe that the diagnostics of  
428 physical similarity, we have described, should become a standard procedure before a phenomenological  
429 model can be utilized for interpretations of historical records or for future predictions. In other words,  
430 claiming a model to be a phenomenological one is not an indulgence but a liability.

431 The results of the analysis are summarized in Fig. 3. Here, the physical similarity is visualized as  
432 proximity between the models in the  $\left(\frac{\varepsilon}{\delta}, V\right)$  space. The positive-versus-negative feedback diagrams  
433 provide additional insight. It can be observed that the original VCV18 and G23 models are very different  
434 from VCV18-1, VDP, and LP22 models not just because the latter may generate 100-kyr cycle without  
435 orbital forcing. The mechanism of ice disintegration is very different in these two groups of models. In  
436 VCV18-1, VDP, and LP22 models, the disintegration of ice sheets happens when the negative feedback  
437 suddenly becomes dominant and destroys an ice sheet. In both VCV18 and G23 models, the  
438 disintegration is due to the additional, fast, positive feedback, which is small during most of the ice-  
439  
440



441 growth period, but eventually becomes strong enough to boost the orbital forcing that attempts ice  
442 destruction.



443

444 **Figure 3.** Physical similarity diagnostics in the  $\frac{\varepsilon}{a} - V$  space for the obliquity-period doubling of the  
445 VCV18 and G23 models and for 100-kyr auto-oscillations of the VDP, LP22, and VCV18-1 models

446 LP22 and G23 models can be considered to be physically similar to particular versions of the VCV18  
447 model, which amounts to saying that they may be derived from basic laws of physics under some  
448 reasonable physical assumptions. These findings boost the physical viability of these phenomenological  
449 models, but this is not unconditional and there are clear boundaries of these phenomenological models  
450 physical legitimacy. For LP22, the ratio of feedback's amplitudes, the V-number, is also the ratio of  
451 timescales. For the Late Pleistocene and for the Early Pleistocene, all timescales are likely to be different  
452 and physical similarity therefore would need to be re-examined for each period separately. For G23  
453 model, physical similarity was found only for the obliquity-range forcing.

454 Generally speaking, our observation that the VDP model is not physically similar to the simplified  
455 version of the VCV18 model is not a final verdict. It is indeed an indication that VDP is not based on *ice*  
456 physics, but there may be other physical phenomena that may provide physical legitimacy to VDP model.  
457 We are a bit skeptical though that such phenomenon can easily be found, because it would need to be  
458 constrained in the same way as VDP is. Specifically, its ratio of positive and negative feedbacks must to  
459 be fixed to a specific value that never changes.

460 As a final conclusion, we agree with Saltzman's (2002) proposal that "the essential slow physics is to  
461 be sought in the low-order models." We observe though that "essential slow physics" that can be derived  
462 from phenomenological models is limited to orbital and terrestrial timescales, to ratios of amplitudes of  
463 orbital and terrestrial forcings, and to ratios of amplitudes of positive and negative feedbacks. This is as  
464 much as phenomenological models can offer, and therefore, we deviate from Saltzman's (2002) further  
465 idea that more explicit models should be tuned to satisfy a best phenomenological model. Instead, we  
466 propose to use available physical models for diagnostics of physical-similarity hypothesis that needs to be  
467 either confirmed or rejected.

468 Of course, encoding empirical data in a simple mathematical statement will always remain a tempting  
469 possibility. As Grigory Barenblatt (2003) said "Applied mathematics is the *art* of constructing  
470 mathematical models of phenomena in nature..." This means that there are no strict rules on how a piece  
471 of mathematical "art" needs to be produced. Therefore, we do not attempt here to discourage our fellow  
472 "artists" from alluding to phenomenological models. Our goal instead was to remind them about  
473 phenomenological models' limitations and to suggest how these limitations may be addressed.



- 474  
475 **Author contributions:** MYV conceived the research (Verbitsky, 2022b), developed the formalism, and  
476 wrote the first draft of the manuscript. The authors jointly discussed the findings and contributed equally  
477 to the editing of the manuscript.
- 478 **Competing interests:** The authors declare that they have no conflict of interest.
- 479 **Acknowledgement:** We are grateful to Andrey Ganopolski for discussions and generous insight into G23  
480 model that includes time series of Fig. 2(c, d), and to Dmitry Volobuev for his help in digitizing VCV18.
- 481 **References**
- 482 Barenblatt, G. I.: Scaling, Cambridge University Press, Cambridge, ISBN 0 521 53394 5, 2003.
- 483 Berger, A. and Loutre, M. F.: Insolation values for the climate of the last 10 million years, *Quaternary*  
484 *Sci. Rev.*, 10, 297–317, 1991.
- 485 Buckingham, E.: On physically similar systems; illustrations of the use of dimensional equations, *Phys.*  
486 *Rev.*, 4, 345–376, 1914.
- 487 Crucifix, M.: Why could ice ages be unpredictable?, *Clim. Past*, 9, 2253–2267,  
488 <https://doi.org/10.5194/cp-9-2253-2013>, 2013.
- 489 De Saedeleer B., Crucifix, M. and Wiczeorek, S.: Is the astronomical forcing a reliable and unique  
490 pacemaker for climate? A conceptual model study, *Climate Dynamics*, (40) 273-294 doi:10.1007/s00382-  
491 012-1316-1, 2013.
- 492 Ganopolski, A.: Toward Generalized Milankovitch Theory (GMT), *Clim. Past*, 19, (to be submitted),  
493 2023.
- 494 Guckenheimer, J., Hoffman, K., and Weckesser, W.: The Forced van der Pol Equation I: The Slow Flow  
495 and Its Bifurcations, *SIAM Journal on Applied Dynamical Systems*, 2, 1-35,  
496 doi:10.1137/S1111111102404738, 2003.
- 497 Haken, H.: Information and self-organization: A macroscopic approach to complex systems. Springer  
498 Science & Business Media, 2006.
- 499 Kaufmann, R. K., and Pretis, F.: Understanding glacial cycles: A multivariate disequilibrium approach.,  
500 *Quaternary Science Reviews* 251, 106694, 2021
- 501 Leloup, G. and Paillard, D.: Influence of the choice of insolation forcing on the results of a conceptual  
502 glacial cycle model, *Clim. Past*, 18, 547–558, <https://doi.org/10.5194/cp-18-547-2022>, 2022.
- 503 Paillard, D.: The timing of Pleistocene glaciations from a simple multiple-state climate model, *Nature*  
504 391, 6665, 378-381, 1998.
- 505 Saltzman, B.: Dynamical paleoclimatology: generalized theory of global climate change, in: Vol. 80,  
506 Academic Press, San Diego, CA, ISBN 0 12 617331 1, 2002.
- 507 Saltzman, B. and Maasch, K. A.: A first-order global model of late Cenozoic climatic change II. Further  
508 analysis based on a simplification of CO<sub>2</sub> dynamics, *Clim. Dynam.*, 5, 201–210, 1991.



- 509 Saltzman, B. and Verbitsky, M. Y.: Asthenospheric ice-load effects in a global dynamical-system model  
510 of the Pleistocene climate, *Climate Dynamics*, 8, 1-11, 1992.
- 511 Saltzman, B. and Verbitsky, M. Y.: Multiple instabilities and modes of glacial rhythmicity in the Plio-  
512 Pleistocene: a general theory of late Cenozoic climatic change, *Climate Dynamics*, 9, 1–15, 1993.
- 513 Saltzman, B. and Verbitsky, M.: Late Pleistocene climatic trajectory in the phase space of global ice,  
514 ocean state, and CO<sub>2</sub>: Observations and theory, *Paleoceanography* 9, 6, 767-779, 1994
- 515 Talento, S. and Ganopolski, A.: Reduced-complexity model for the impact of anthropogenic CO<sub>2</sub>  
516 emissions on future glacial cycles, *Earth Syst. Dynam.*, 12, 1275–1293, [https://doi.org/10.5194/esd-12-](https://doi.org/10.5194/esd-12-1275-2021)  
517 1275-2021, 2021.
- 518 Tzedakis, P.C., Crucifix, M., Mitsui, T. and Wolff, E.W.: A simple rule to determine which insolation  
519 cycles lead to interglacials. *Nature*, 542(7642), 427-432, 2017
- 520 Tziperman, E., Raymo, M. E., Huybers, P., and Wunsch, C.: Consequences of pacing the Pleistocene  
521 100 kyr ice ages by nonlinear phase locking to Milankovitch forcing, *Paleoceanography*, 21, PA4206,  
522 <https://doi.org/10.1029/2005PA001241>, 2006.
- 523 van der Pol, B.: On oscillation hysteresis in a triode generator with two degrees of freedom, *Philosophical*  
524 *Magazine Series* 6, 43, 700—719, doi:10.1080/14786442208633932, 1922.
- 525 Verbitsky, M. Y.: Inarticulate past: similarity properties of the ice–climate system and their implications  
526 for paleo-record attribution, *Earth Syst. Dynam.*, 13, 879–884, <https://doi.org/10.5194/esd-13-879-2022>,  
527 2022a.
- 528 Verbitsky, M.: Do phenomenological dynamical paleoclimate models have physical similarity with  
529 nature?, *EGUsphere* [preprint], <https://doi.org/10.5194/egusphere-2022-758>, 2022b
- 530 Verbitsky, M. Y. and Chalikov, D. V.: *Modelling of the Glaciers-Ocean-Atmosphere System*,  
531 *Gidrometeoizdat, Leningrad*, edited by: Monin, A. S., 135 pp., 1986.
- 532 Verbitsky, M. Y. and Crucifix, M.:  $\pi$ -theorem generalization of the ice-age theory, *Earth Syst. Dynam.*,  
533 11, 281–289, <https://doi.org/10.5194/esd-11-281-2020>, 2020.
- 534 Verbitsky, M. Y. and Crucifix, M.: ESD Ideas: The Peclet number is a cornerstone of the orbital and  
535 millennial Pleistocene variability, *Earth Syst. Dynam.*, 12, 63–67, [https://doi.org/10.5194/esd-12-63-](https://doi.org/10.5194/esd-12-63-2021)  
536 2021, 2021.
- 537 Verbitsky, M. Y., Crucifix, M., and Volobuev, D. M.: A theory of Pleistocene glacial rhythmicity, *Earth*  
538 *Syst. Dynam.*, 9, 1025–1043, <https://doi.org/10.5194/esd-9-1025-2018>, 2018.